Proceedings of the Korean Nuclear Society Spring Meeting
Gyeong ju, Korea, May 2003

Viscous Fluid Motion Simulation by MARS 3D Module

Sung Won Bae, Jae-Jun Jeong, Bub Dong Chung

Korea Atomic Energy Research Institute
150 Dukjin-dong, Yuseong-gu
Daejun 305-353, Korea

Abstract

The MARS code is a best-estimation program which is based on the RELAP5 and COBRA-TF codes. The dominant usage of MARS code is to analyze the transient behavior of the thermal-hydraulic systems. MARS code provides the multi-dimensional modeling capabilities by means of COBRA-TF based 3D module. MARS 3D Module shows appropriate applications when it is used to model a vertical flow dominant channel flows, especially. In spite of this reliability, one weak point of MARS 3D module is that there is no way to represent any viscous fluid flow interpretations. For the viscous fluid flow interpretations, MARS code has been modified so that it can accept zero-perimeter channel input. It is also modified to include dynamic and turbulent shear stress term in the directional momentum conservation equation sets. The turbulent viscosity is calculated by Prandtl's Mixing Length assumption. For the assessment, an expanding vertical pipe flow and a short square channel flow are selected. The results are compared to FLUENT analysis obtained with standard k-ε turbulent model. The viscous motion effect of single phase water is simulated. In the simulation view points, the bulk flow induced by viscosity is reasonably included.

1. INTRODUCTION

There have been many trials to include the turbulence interpretations in nuclear power plant system analysis codes. COBRA code has many representative examples. As the earlier case of trials, COBRA had been tried to include turbulence model with fine grid analysis of steam generator. But the benefits of including the viscous fluid flow and turbulence was inconsiderable compared to the calculation cost and modeling efforts. After 1986, COBRA code intended to interpret the effect of turbulence only instead of the turbulence itself. The effect of turbulence is bubble accumulation phenomena, so called void drift, during the two phase flow of vertical sub channels. In that case, the viscous fluid motion is out of considerations. The void drift method is a correlation model of cross flow rate to the axial

dominant flow rate. This model accounts for the fact that the cross flow mixing is enhanced by the motion of accumulated vapor bubbles along the vertical flow passages.

As shown in Table 1, it is difficult to include the viscous and turbulence effect in thermal hydraulic system simulation program. It is the tendency to replace the turbulent and dynamic viscosity analysis with the simple modeling of the effect of turbulent flow phenomena.

Nevertheless, there still exists the need not to neglect the effect of viscous and turbulence effects. A large water reservoir like IRWST may be modeled and simulated by only a volume with current one dimensional simulation programs. The MARS 1D module is not exceptional. When an IRWST is modeled as a 1D volume, it is impossible to show the internal fluid flow behavior and temperature distribution as the hot steam inflows to the volume. MARS 3D module has the ability to model the bulk reservoir as a set of multiple channels. But it provides the spatial division. It has no way to simulate the fluid motion resulting from the turbulent and dynamic viscosity of fluids.

RELAP5-3D [7] also provides the ability to model a volume with the grids. It has the restriction to analyze the turbulent behavior of fluid because the coarse grid characteristics.

Consequently, it is needed to have an ability to simulate the fluid motion in a large volume of space as a pre process of detail analysis of an interesting volume component.

Table 1. Summary of Viscous Stresses and Turbulent Modeling in Several Versions of COBRA Code

Ref. / Year	Viscous stress model	Turbulence model	Comments
1 / 1980	Axial & lateral momentum equations for liquid phase only.	Mixing length model, Momentum & energy equations for liquid-phase.	Two-fluid model, SG analysis. Micro-scale modeling.
2 / 1982	Axial & lateral momentum equations for liquid and vapor phases.	Mixing length model, Momentum & energy equations for liquid- & vapor-phases.	Three-field model. Reactor vessel T/Hs.
3 / 1985	Continuous phase momentum equation only. Treated as in single-phase flow.	Mixing length model, Continuous phase momentum and energy equation.	Three-field model with NC gases. Nuclear containment analysis.
4 / 1986	None	Inter-subchannel mixing coefficient approach in rod bundle geometry. Void drift model. Energy & momentum equations.	Three-field model with NC gases. FLECHT SEASET program.
5 / 1990*	None	“	*year of KAERI acquisition
6 / 1999*	None	“	*year of KAERI acquisition

2. IMPLEMENTATION OF TURBULENT VISCOSITY

The discrete momentum equation used in MARS 3D has no viscosity terms. Instead, wall friction and form drag coefficient are assigned by the gap input. These two input parameters are used to calculate the pressure drop through the channel components. In the conventional use of the MARS 3D module, the value of form drag coefficient depends on the geometry of the flow path modeled by the gap. A value of 0.5 is typically used for flow across one row of rods or tubes. For gaps that are formed by vessel walls rather than rod arrays, the pressure loss in the gap is primarily a friction loss rather than a form loss. Wall friction factors in a gap are computed internally in the code according to the user specified coefficient. If this value is zero, no wall friction is calculated. If the channel faces wall on one side and two sides, the values are 0.5 and 1.0, respectively.

With these parameters, only the overall velocity head loss is computed. It is impossible to see the fluid movements caused by viscous fluidic shear. In order to overcome this restriction, shear force term is added in discrete momentum equation in MARS 3D module. The modified discrete momentum equation for liquid phase containing shear force term is represented below:

$$\frac{\left[(arU)_j^n-(arU)_j\right]A_{mj}}{\Delta t}=\{1\}+\{2\}+\{3\}+\{4\}+\{5\}+\{6\} \tag{1}$$

$$\{1\}=\frac{\sum_{KB=1}^{NB}\left[(arU)^*U_j\right]_{KB}A_{mKB}}{\Delta x_j}-\frac{\sum_{KA=1}^{NA}\left[(arU)^*U_{j+1}\right]_{KA}A_{mKA}}{\Delta x_j}$$

$$\{2\}=\sum_{LB=1}^{NKB}\left[(arU)^*V_J\right]_{LB}\frac{S_{LB}}{2}+\sum_{LA=1}^{NKA}\left[(arU)^*V_{J+1}\right]_{LA}\frac{S_{LA}}{2}$$

$$\{3\}=-(ar)_j gA_{mj}-\frac{(P_{J+1}-P_J)^n}{\Delta x_j}a_j A_{mj}$$

$$\{4\}=-K_j\left(2U_j^n-U_j\right)+K_{Vj}\left[2(U_V-U)_j^n-(U_V-U)_j\right]$$

$$\{5\}=\frac{(1-h)(\Gamma_C U_V-\Gamma_E U)_j}{\Delta x_j}+\frac{(S_D U_E-S_E U)_j}{\Delta x_j}+\frac{S_{mj}}{\Delta x_j}$$

$$\{6\}=T_j^T$$

The first two terms are axial change of convective momentum. The terms in {2} mean the lateral convective momentum changes. Terms in {3} are for gravitation and pressure gradient terms. Terms in {4} mean the combined drag and frictional momentum decrease and phase interface shear. Terms in {5} mean the momentum change caused by mass transfer. MARS 3D include droplet entrainment field as a system variable. Last term {6} means the fluidic shear stress term. The same equation set is prepared for vapor and entrainment phases. Further, lateral direction momentum equation is dealt in another 3 equation sets. Adequate

form of fluidic shear term is added in each equation set. For the axial momentum equation for liquid phase, the detail form of fluidic shear term is represented in equation (2). The *NSUR* means the number of surrounding meshes.

$$T_j^T = \sum_{SUR=1}^{NSUR} (a r)_j (m + m_T) \frac{U_j - U_{SUR}}{\Delta L_{SUR}} \tag{2}$$

Here, the turbulent viscosity, m_T, is calculated by the Prandtl's Mixing Length Theory,

$$m_T = r \lambda^2 \sum_{SUR=1}^{NSUR} \left| \frac{\Delta U}{\Delta L} - \frac{\Delta V}{\Delta x} \right|_{SUR} / NSUR \tag{3}$$

The velocity gradients across the axial nodes and lateral gaps surrounding a channel mesh are computed and averaged. The turbulent length scale λ is the most important parameter in order to perform a reasonable flow simulation. The value for the length scale is based on the user input. Table 2 shows the useful length scales for several simple geometries [8].

Table 2. Turbulent length scale for simple flow geometry

Flow	Turbulent length scale, λ	Length scale, L
Mixing layer	0.07 L	Layer width
Jet	0.09 L	Jet half width
Wake	0.16 L	Wake half width
Axisymmetric jet	0.075 L	Jet half width
Boundary layer Viscous sub-layer Log-law layer Outer layer	0.09 L	Boundary layer thickness
Channel	$L\left[0.14 - 0.08(1 - y/L)^2 - 0.06(1 - y/L)^4\right]$	Channel half width

3. FLOW SIMULATION WITH TURBULENT VISCOSITY

3.1 Modeling an Expansion Pipe

For the viscous flow simulation, it is basically required to divide a volume or flow path to many grids or meshes. But current 1D modeling components represent the flow domain inside a wall or heat structure. Even in MARS 3D module, it is usual to model a vessel with a concept that the heat structure or wall should be a boundary of the vessel model. When a small channel exists inside a large channel without a physical boundary, it is also required to

input the wetted perimeter. The wetted perimeter and channel flow area are the parameters to calculate the hydraulic diameter of the small channel. Therefore, it means that the enveloping large channel and inside small channel are fully separated with the fluidic motion point of view.

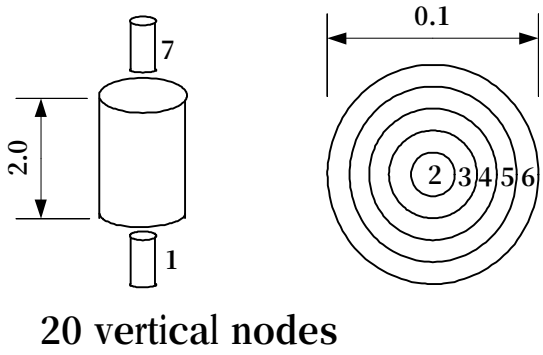

Inlet flow rate : 1.0 kg/s
Condition : 15.0 Mpa, 600 K

Channel	Area(m^2)	Perimeter(m)
1	0.000314	0.06283
2	0.000314	0.06283
3	0.000942	0.18850
4	0.001571	0.31416
5	0.002199	0.43982
6	0.002827	0.56549
7	0.000314	0.06283

Fig. 1. Vertical expansion pipe model

Figure 1 shows the vertically configured pipe initially filled with subcooled water at 15.0 MPa and 600 K. The flow rate of subcooled water is 1.0 kg/s at the same condition. Pipe diameter is 0.1 m and length is 2.0 m. It has narrow inlet and outlet. The diameter of inlet and outlet is 0.02 m. This pipe is modeled by 5 channel components which are annular forms. These 5 annular channels are arranged coaxially and make the shape of a pipe. The inner and outer radius of each annular channel increases by 0.01 m.

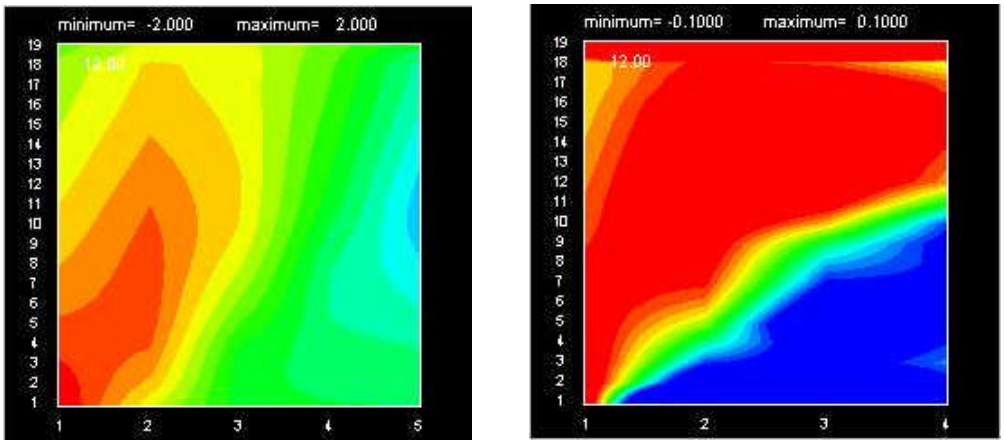

(a) Axial direction (b) Lateral direction

Fig. 2. Contour of mass flow rate (kg/s) in axial and lateral direction of vertical expansion pipe flow; conventional non-zero MARS 3D channel perimeter input results.

Following the conventional non-zero perimeter input, the original MARS 3D recognizes each channel separately. It means that all channels have its own hydraulic diameter independently. In other words, original MARS 3D finds no differences from the nodalization

of the channels that are positioned in side by side. Figure 2 shows the results obtained by the original MARS 3D without the turbulent shear term. In this case, main flow is derived by pressure difference between each neighboring channels. In Fig. 2 (b), The apposite lateral flow directions are evenly sharing the flow domain. Considering the real dimension of the pipe length, the expansion region possesses abnormally long range of the pipe. Also considering that the plot variable is mass flow rate, most flow is concentrated in the pipe center region. This is the same to the typical result of the case that the channels are connected in serial configurations and the area of each channels are increasing.

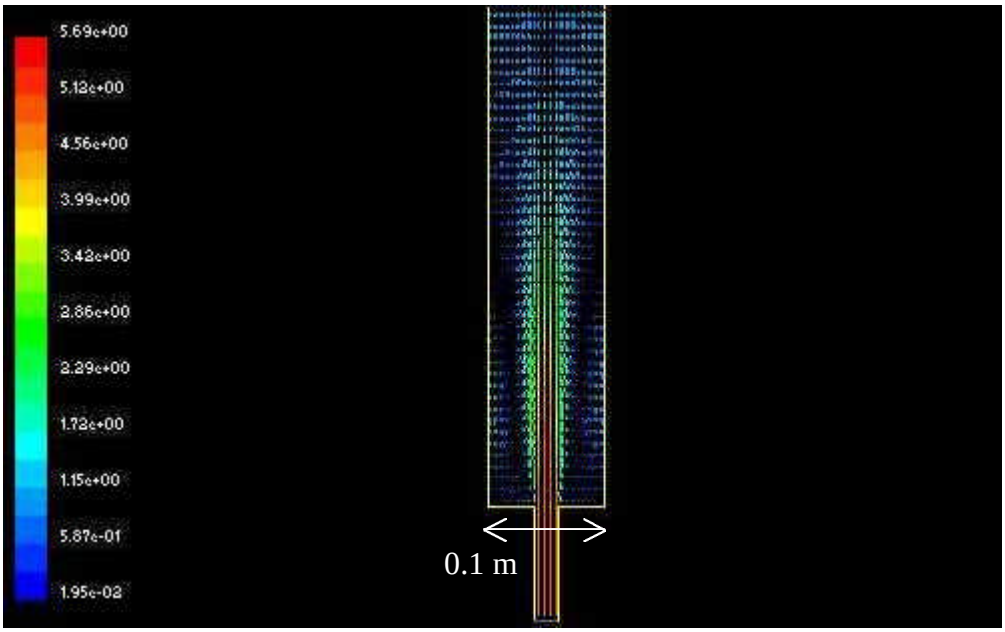

Fig. 3. The axial velocity plot of vertical expansion pipe solved by FLUENT 6.0.

Because the viscous fluidic motion acts like a mechanism of momentum diffusion, the concentration of flow might be eliminated in the fully developed region. Figure 3 reasonably shows the flow averaging action of the turbulence and viscosity of fluid near the pipe inlet region. The results are obtained with FLUENT 6.0. The standard k-ε turbulence model is applied. The grid numbers are 200 and 34 for axial and lateral direction, respectively. The expansion flow has the typical turbulent velocity profiles and fully develops the flat shape near the 0.5 m down stream from the pipe inlet. Axial reverse flow also is observed at the pipe corner regions.

The undesired recognition and analysis of channel system of original MARS 3D comes from the non-zero perimeter input of channels. In order to overcome the non-zero input restriction, original MARS 3D has been modified to access the zero perimeter channels. If the input value of perimeter is 0.0, it is required to put the user defined hydraulic diameters.

Figure 4 shows the modified MARS 3D result of the case that the zero perimeter input is permitted. In this case, user input hydraulic diameter for all channels are set to 0.1. The channel 6 uses its own perimeter, 0.31416m. The strong lateral direction flow is observed up to the 0.5 m downstream. For axial direction, reverse flow is observed, too. Beyond the inlet region, axial flow is evenly distributed through the cross section. Figure 5 shows the upward

axial velocity along the radial positions at the location of 0.2 and 0.4 m from the inlet. The results of FLUENT 6.0 and modified MARS 3D are compared to show a reasonable viscous fluidic motion simulation. At the 0.2 m downstream, as in Fig. 5 (b), even an axial reverse flow is revealed by MARS 3D.

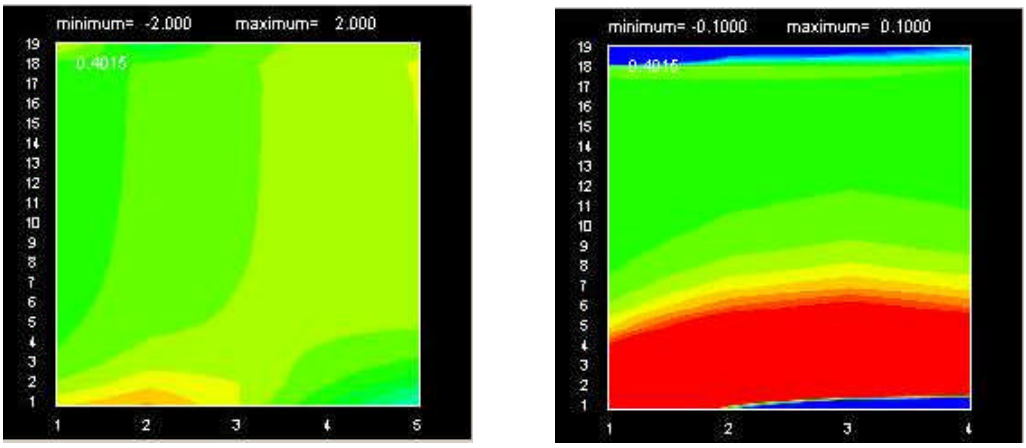

(a) Axial direction (b) Lateral direction

Fig. 4. Contour of mass flow rate (kg/s) in axial and lateral direction of vertical expansion pipe flow; modified MARS 3D with zero channel perimeter input results.

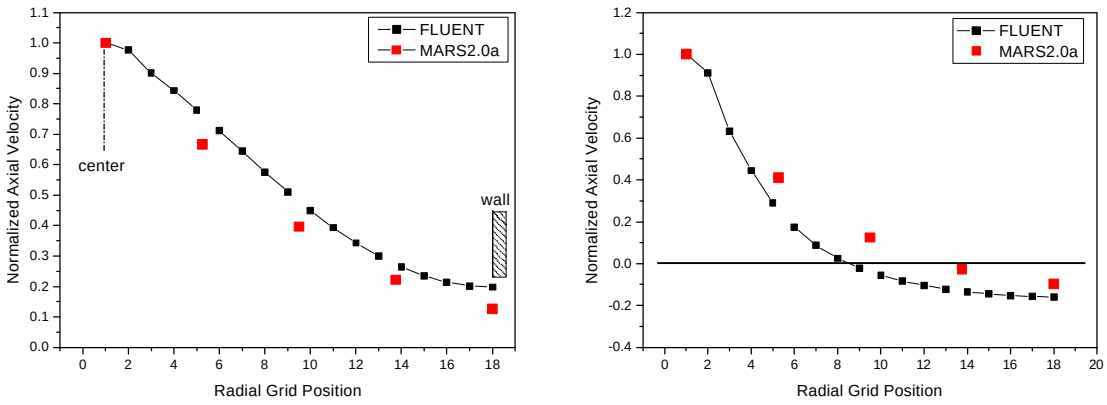

(a) 0.4 m downstream from the inlet (b) 0.2 m downstream from the inlet

Fig. 5. Comparisons of axial velocity along the radial positions between FLUENT 6.0 and modified MARS 3D results.

3.2 Modeling a Short Square Block

Using the same concept of the expansion pipe, the short square block is modeled into 20 sub channels. The nodalization is shown in Fig. 6. In that figure, main block is section 2. For all sub channels, one side length is assigned to 0.1 m. 6 internal channels have zero perimeters. Instead, they have the user specified hydraulic diameter as 0.8 m. The main block

channel length is 0.6 and divided into 12 nodes. Inlet mass flow is 2.0 kg/s and the condition are 15.0 MPa and 600K.

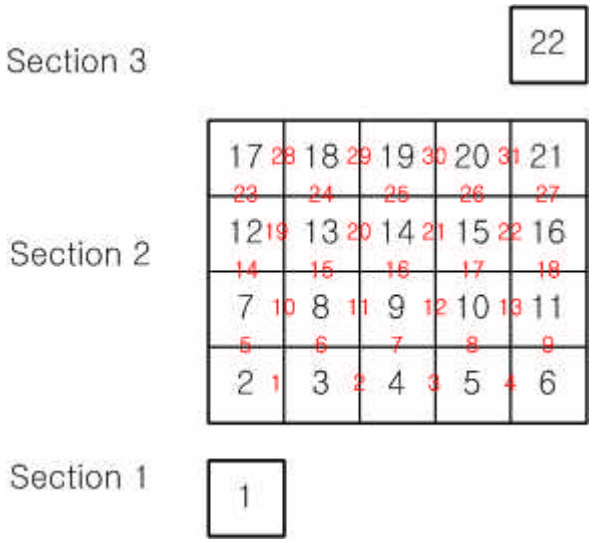

Fig. 6. Nodalization of channel and gap for the short square block.

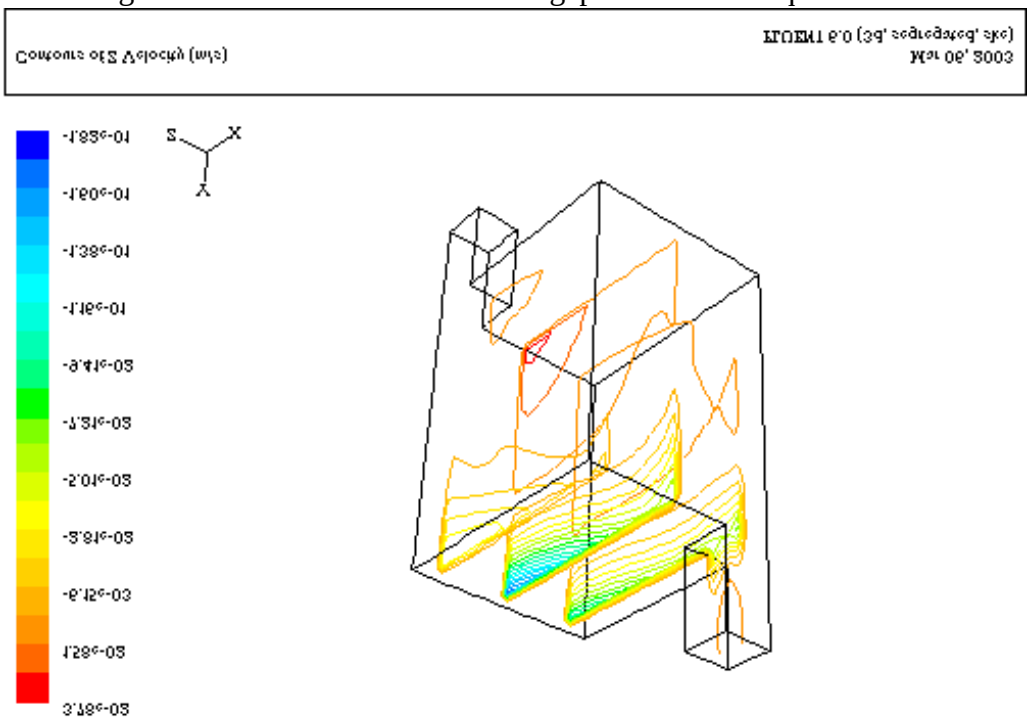

Fig. 7. Contour of z-direction velocity solved by FLUENT 6.0 for short square block.

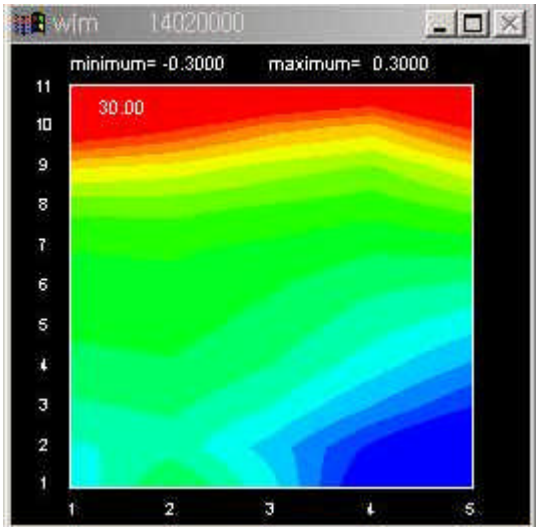

Fig. 8. The gap flow rate plot at equivalent position to the middle plane of Fig. 7.

In this case, it is important to treat the orthogonal configuration of gaps. Strictly speaking, coaxial expansion pipe is only 2 dimensional simulation of flow because there is no q coordinate. But in this example, sub channels build up a full 3 dimensional volume. Therefore, additional input required for defining the relative location of 20 sub channels and 31 gaps. MARS 3D provides NLMGAP input system for the orthogonal configuration.

In Fig. 7, the z-directional velocity contour is shown obtained by FLUENT 6.0. FLUENT model generates the meshes with 0.02 m grid size for whole domain. The standard k-ε turbulent model is adopted again in this case. It is interesting that the reverse flow is observed at the lower side near the inlet of the block. For the comparison, the lateral velocities for the gaps 14, 15, 16, 17 and 18 are plotted. The results of modified MARS 3D reveal a reversed flow at the lower away side of block. The location of reverse flow occurs is different from each case. But, in the upper side of block, there are strong lateral flows in both cases. For the detail quantitative comparison, the user input hydraulic diameter should be considered precisely. Also, it should be noted that the maximum available grid size might exist.

4. CONCLUSION

The viscous shear stress terms are added in the momentum equation sets of the MARS 3D module. This modified MARS 3D module is able to accept zero perimeter channels and user defined hydraulic diameters. In addition to these new input features, shear stress involved MARS 3D makes it possible to see the fluidic motion in a bulk two- or three-dimensional volumes. In spite of some successful results, a few tasks are remained unresolved.

The user defined hydraulic diameter makes serious effects onto the simulation results. The reasonable channel or mesh size should be recommended, too. These tasks are connected and coupled to each other. It is also required to interpret the interactions between the heat structures and shear induced flow.

It is noted that the modified MARS 3D suggests only simulation results rather than

arithmetic analysis results. Therefore, it might be emphasized that the usage of MARS 3D module is helpful for the case of qualitative level of flow simulation or pre-process of CFD analysis.

Acknowledgement

We are grateful to the Ministry of Science and Technology of Korea to fully support this research of the Long-and-Mid-Term Nuclear R & D Program.

REFERENCES

1. C.W. Stewart, J.S. Barnhart, and A.S. Koontz, Improvements to the COBRA-TF (EPRI) Computer Code for Steam Generator Analysis, EPRI NP-1509 (1980).
2. M.J. Thurgood and T.L. George, COBRA/TRAC – A Thermal-Hydraulics Code for Transient Analysis of Nuclear Reactor Vessels and Primary Coolant Systems, NUREG/CR-3046 (1982).
3. M.J. Thurgood and T.L. George, COBRA-NC Workshop Presentation Materials, COBRA-NC Workshop (June 1985).
4. C.Y. Paik, L.E. Hochreiter, J.M. Kelly and R.J.Kohrt, Analysis of FLECHT SEASET 163-Rod Blocked Bundle Data Using COBRA-TF, EPRI NP-4111 (NUREG/CR-4166) (1986).
5. COBRA-TF Source Program in MARS (1990).
6. COBRA-TF Source Program in WCOBRA/TRAC (1999).
7. RELAP5-3D Code Manual Volume I: Code Structure, System Models and Solution Methods, INEEL-EXT-98-00834, Idaho National Engineering and Environmental Laboratory (July 2002).
8. K. K. Versteeg and W. Malalasekera, An Introduction to Computational Fluid Dynamics, LONGMAN (1995).